Efficient Dynamic Compressor Optimization
in Natural Gas Transmission Systems

Terrence W. K. Mak, Pascal Van Hentenryck, Anatoly Zlotnik, Hassan Hijazi, and Russell Bent

Abstract— The growing reliance of electric power systems on gas-fired generation to balance intermittent sources of renewable energy has increased the variation and volume of flows through natural gas transmission pipelines. Adapting pipeline operations to maintain efficiency and security under these new conditions requires optimization methods that account for transients and that can quickly compute solutions in reaction to generator re-dispatch. This paper presents an efficient scheme to minimize compression costs under dynamic conditions where deliveries to customers are described by time-dependent mass flow. The optimization scheme relies on a compact representation of gas flow physics, a trapezoidal discretization in time and space, and a two-stage approach to minimize energy costs and maximize smoothness. The resulting large-scale nonlinear programs are solved using a modern interior-point method. The proposed optimization scheme is validated against an integration of dynamic equations with adaptive time-stepping, as well as a recently proposed state-of-the-art optimal control method. The comparison shows that the solutions are feasible for the continuous problem and also practical from an operational standpoint. The results also indicate that our scheme scales to large gas transmission networks with more than 6000 kilometers of total pipeline.

I. INTRODUCTION

In the last two decades, the increasing integration of renewable sources of energy in the electrical power system, together with the recent availability of natural gas in the United States, acted as a primary driver of installation of gas-fired electric power plants to meet most of the demand for new generating capacity [1]. Gas-fired generators may go online and shut down several times a day, and can rapidly modify their outputs, making them attractive generation resources to balance the fluctuations of renewable energy sources such as wind and solar [2], [3].

Historically, withdrawals from natural gas transmission systems came from utilities and industrial consumers, which are highly predictable and exhibit low variation in demand [4]. These withdrawals are traded using day-ahead contracts for fixed deliveries and implicilty assume that injections and withdrawals remain nearly constant. As a result, natural gas transmission systems could be largely controlled and optimized using steady-state modeling [5], [6]. Early studies [7], [8], [5] focused on optimizing steady-state gas flows, for which the state equations are algebraic relations. Recent

efforts have improved and scaled up optimization techniques for similar problems [9], [10], [11], [12], [13]. In short-term operations, the operating set-points for gas compressor stations can be readily changed, and compressor optimization for steady-state flows has been solved in the form of an optimal gas flow (OGF) [11].

However, it is no longer appropriate to restrict attention to steady-state approximations, which cannot adequately describe the physics of high volume gas flows that may fluctuate significantly throughout the day according to gas-fired generator dispatch and commitment schedules [14], [15]. Recent studies have highlighted the challenges created by such increasing flow variability and volume [16], which are predominantly caused by the growing use of gas-fired power plants for electricity generation [1], [17]. The integration issues that face the increasingly interdependent electric and gas systems have created growing concerns in both industry sectors [3]. As a result, in order to enable natural gas systems to inter-operate with electric power systems on the time-scale of generator dispatch, the OGF must be extended to account for transient flow conditions. *Therefore, new optimization techniques that use dynamic models of gas flows on pipeline networks are required* [18].

An automatic control methodology for optimally managing transient flows in gas transmission systems will require a stable, accurate, physics-based, and rapid technique for computing model-based compressor control protocols. Automatic grid control tools are already industry standards for management of generator dispatch for electric power systems [19]. Such power system optimization models consider one or a sequence of steady states [20][1], but the significant qualitative difference in the physics of gas pipeline networks prevents these techniques from being directly transferred. Indeed, the dynamics in the electricity and gas networks operate at fundamentally different space and time scales.

Gas pipeline flow dynamics on the relevant spatial and temporal scales do not experience waves or shocks, and can be represented by the Euler equations for compressible gas flow in one-dimension with significant simplifications [23], [24]. These partial differential equations (PDEs) are highly nonlinear, however, and are challenging to simulate [25], particularly when instances over many domains are coupled at the boundaries over a network. This nonlinearity and complexity of gas pipeline network dynamics is also an obstacle to tractable optimization of such flows

T. W. K. Mak and H. Hijazi are at NICTA and Australian National University, Canberra, ACT, Australia. Email: {Terrence.Mak | Hassan.Hijazi}@nicta.com.au; P. Van Hentenryck is at the Department of Industrial & Systems Engineering, University of Michigan, Ann Arbor, MI, USA. Email: pvanhent@umich.edu; R. Bent and A. Zlotnik are at Los Alamos National Laboratory, Los Alamos, NM, USA. Email: {rbent | azlotnik}@lanl.gov.

under transient conditions. Several studies have proposed optimization schemes for gas networks on the time-scale of daily operations. These approaches used high fidelity simulation that made gradient information costly to obtain [26], or relied on specialized structures [27], [28]. Recent studies investigated stochastic optimization as well [29]. A recent method relied on a lumped-element method for spatial discretization and a pseudospectral collocation scheme in time [30]. *In all these studies, the issues of computation time and scalability have been noted repeatedly.*

In this manuscript, we consider the Dynamic Optimal Gas Flow (DOGF) problem, which generalizes the OGF to capture the dynamics of a gas pipeline network. The objective of the DOGF is to minimize the cost of gas compression required for pipeline operations subject to system pressure constraints, and whose deliveries to customers are described by time-dependent mass flow. *Our main contribution is an efficient optimization scheme for the DOGF, which is validated by an accurate simulation method for gas pipeline networks with dynamic flows and compressors.*

The key aspects of our optimization scheme can be summarized as follows. First, following [30], the hydro-dynamic relations that describe gas flow are discretized in time and space using first order approximations, and several relaxations of the resulting nonlinear constraints are employed. Second, in contrast to earlier work that was based on pseudospectral discretization, our proposed scheme uses a trapezoidal discretization but compensates for the potential loss in accuracy by a two-stage optimization approach. In the first stage, our scheme optimizes the compression cost (the original objective). In order to obtain a physically realistic solution, the second stage optimizes the smoothness of the compressor ratios while ensuring that the overall compression costs remain close to the value found in the first stage. The resulting large-scale nonlinear optimization problems (with up to more than 130,000 decision variables) are solved using the state-of-the-art IPOPT system [31], enabling us to exploit the significant progress in nonlinear optimization in the last decades.

The solutions produced by our optimization scheme are verified in two ways:

1) By comparing them to a validated dynamic simulation method for gas pipeline networks with transient compression [32], [33], which is seeded with the compressor ratios of our optimized solutions; and
2) By comparing them to the state-of-the-art method for the DOGF.

The validation process indicates that our optimization scheme produces solutions with no pressure violations and with physically meaningful mass flow and pressure trajectories in the corresponding simulation. Moreover, the compressor ratios in our solutions only have negligible differences compared to the state-of-the-art method. The main benefit of our optimization scheme, however, is its computational efficiency: Compared to earlier approaches, *it reduces solution times up to an order of magnitude*. In particular, it solves a previously investigated 24-pipe gas network case

study in less than 30 seconds and demonstrates scalability on networks with 24, 40 and 135 pipes, with total pipeline lengths of 477, 1118, and 6964 kilometers, respectively.

The rest of the paper is organized as follows. Section II summarizes the physical modeling of gas pipeline networks and poses the DOGF. Section III describes the discretization scheme and relaxations required for an efficient optimization formulation. Section IV presents our two-stage optimization approach and implementation details, followed by computational results for the three case studies, including convergence experiments and validating simulations. Section V concludes with a discussion and future extensions.

II. COMPRESSOR OPTIMIZATION IN GAS PIPELINES

A gas pipeline network can be represented as a directed graph $\mathcal{G} = (\mathcal{J}, \mathcal{P})$, where edges $\{i, j\} \in \mathcal{P}$ represent pipes P_{ij} that connect nodes $i, j \in \mathcal{J}$ that represent joints J_i and J_j. The dynamic state on the pipe P_{ij} is given by pressure p_{ij} and mass flow q_{ij}, which evolve on a time interval $[0, T]$ and the distance variable $x_{ij} \in [0, L_{ij}]$, where L_{ij} is the length of pipe P_{ij}. We are interested in the subsonic and isothermal regime of transients that do not excite shocks or waves, i.e., where the flow velocity through a pipe is less than the speed of sound a in the gas, and temperature is assumed to be constant. The flow dynamics on a single pipe P_{ij} can be adequately described in this regime [24] by

$$\frac{\partial p_{ij}}{\partial t} + \frac{a^2}{A_{ij}} \frac{\partial q_{ij}}{\partial x} = 0 \qquad (1)$$

$$2p_{ij} \frac{\partial p_{ij}}{\partial x} + \frac{\lambda a^2}{D_{ij} A_{ij}^2} q_{ij} |q_{ij}| = 0 \qquad (2)$$

The parameters for each pipe P_{ij} are the pipe diameter D_{ij} and cross-sectional area A_{ij}, and the speed of sound a and friction factor λ are assumed uniform and constant throughout the system. The second term in (2) approximates friction effects. The gas dynamics on a pipeline segment are represented using (1)-(2) and possess a unique solution when any two of the boundary conditions $p_{ij}(t, 0)$, $q_{ij}(t, 0)$, $p_{ij}(t, L_{ij})$, or $q_{ij}(t, L_{ij})$ are specified. For both computational and notational purposes, we apply a transformation to dimensionless variables [24] given by

$$\tilde{p}_{ij} = \frac{p_{ij}}{p_N}, \qquad\qquad \tilde{q}_{ij} = \frac{q_{ij}}{q_N}, \qquad (3)$$

$$\tilde{x}_{ij} = x \frac{\lambda a^2 q_N^2}{D_{ij} A_{ij}^2 p_N^2}, \qquad \tilde{t}_{ij} = t \frac{\lambda a^4 q_N^3}{D_{ij} A_{ij}^3 p_N^3},$$

where p_N and q_N are scaling constants. This results in the dimensionless equations

$$\frac{\partial p_{ij}}{\partial t_{ij}} + \frac{\partial q_{ij}}{\partial x_{ij}} = 0, \qquad (4)$$

$$2p_{ij} \frac{\partial p_{ij}}{\partial x_{ij}} + q_{ij} |q_{ij}| = 0, \qquad (5)$$

where we omit the $\sim$ label over the variables for readability. Note that the space and time variables x_{ij} and t_{ij} are now pipe-dependent. We write these variables as x and t when it is clear from the context that they correspond to a specific

pipe P_{ij}. Design limits and regulations for pipeline systems require pressure to remain within specified bounds given by

$$\underline{p}_{ij} \le p_{ij}(t,x) \le \overline{p}_{ij}. \quad (6)$$

The momentum dissipation due to the friction term in (2) causes the gas pressure to decrease, hence it must be augmented by compressors to maintain the minimum required pressure. We define $\mathcal{C} \subset \mathcal{P}$ as the subset of pipes that have compressors. The action of compressors is modeled as conservation of flow and an increase in pressure at a point $c_{ij} \in [0, L_{ij}]$ by a multiplicative ratio $R_{ij}(t) > 0$ that may depend on time. Specifically,

$$\lim_{x \searrow c_{ij}} p_{ij}(t,x) = R_{ij}(t) \lim_{x \nearrow c_{ij}} p_{ij}(t,x), \quad (7)$$

$$\lim_{x \searrow c_{ij}} q_{ij}(t,x) = \lim_{x \nearrow c_{ij}} q_{ij}(t,x). \quad (8)$$

The cost of compression S_{ij} is proportional to the required power [11], and is approximated by

$$S_{ij}(t) = \eta^{-1} |q_{ij}(t, c_{ij})| (\max\{R_{ij}(t), 1\}^{2K} - 1) \quad (9)$$

with $0 < K = (\gamma - 1)/\gamma < 1$, where γ is the heat capacity ratio and η is a compressor efficiency factor. In this study we do not consider pressure regulation (decompression), so the compressor ratio for a given station must remain bounded within a feasible operating region

$$\max\{\underline{R}_{ij}, 1\} \le R_{ij} \le \overline{R}_{ij}. \quad (10)$$

In addition to the dynamic equations (4)-(5) and continuity conditions for compressors (7)-(8) that characterize the system behavior on each pipe $P_{ij} \in \mathcal{P}$, we specify balance conditions for each joint $J_i \in \mathcal{J}$. We first define variables for the unique nodal pressure $p_i(t)$ at each junction, as well as mass flow injections $d_i(t)$ from outside the system (negative for consumptions/withdrawals). Each joint $J_j \in \mathcal{J}$ then has a flow balance condition

$$\sum_{J_i \in \mathcal{J}: P_{ij} \in \mathcal{P}} q_{ij}(t, L_{ij}) - \sum_{J_k \in \mathcal{J}: P_{jk} \in \mathcal{P}} q_{jk}(t, 0) = f_j(t), \quad (11)$$

as well as a pressure continuity condition

$$p_{ij}(t, L) = p_j(t) = p_{jk}(t, 0), \quad (12)$$
$$\forall J_i, J_k \in \mathcal{J} \text{ s.t. } P_{ij}, P_{jk} \in \mathcal{P}.$$

A subset of the junctions $\mathcal{S} \subset \mathcal{J}$ may be treated as "slack" nodes, which reasonably represent large sources of gas to a transmission system. For these junctions, the mass inflow $f_i(t)$ is a free variable and the nodal pressure is a parameter

$$p_i(t) = s_i(t). \quad (13)$$

For the remaining junctions, which reasonably represent consumers or small suppliers of gas to the system, the nodal pressure $p_i(t)$ free and the mass inflow is a parameter

$$f_i(t) = d_i(t). \quad (14)$$

The optimization problem that we aim to solve involves a gas pipeline network for which the conditions at each joint are parameterized by an injection/withdrawal $d_i(t)$ or supply pressure $s_i(t)$. The design goal is for the system to deliver all of the required flows $d_i(t)$ while maintaining feasible system pressure given the physics-based dynamic constraints, and the objective is to minimize the cost of compression over a time interval $[0, T]$. This cost objective is given by

$$C = \sum_{P_{ij} \in \mathcal{C}} \int_0^T S_{ij}(t) \mathrm{d}t. \quad (15)$$

In this study we consider time-periodic boundary conditions on the system state and controls, i.e.,

$$p_{ij}(0,x) = p_{ij}(T,x), q_{ij}(0,x) = q_{ij}(T,x), \forall P_{ij} \in \mathcal{P} \quad (16)$$
$$R_{ij}(0) = R_{ij}(T), \quad \forall P_{ij} \in \mathcal{C} \quad (17)$$

and therefore feasible parameter functions also must satisfy $d_i(0) = d_i(T)$ and $s_i(0) = s_i(T)$. The formulation is

$$
\begin{aligned}
\min \quad & C \text{ in } (15) \\
s.t. \quad & \text{pipe dynamics: } (4), (5) \\
& \text{compressor continuity: } (7), (8) \\
& \text{joint conditions: } (11), (12) \\
& \text{density \& compression constraints: } (6), (10) \\
& \text{periodicity constraints: } (16), (17) \\
& \text{injection parameters: } (13), (14) \\
& \text{compressor power: } (9)
\end{aligned}
\quad (18)
$$

In the next section, we describe a spatial and temporal discretization scheme and relaxation conditions that facilitate efficient solution of this PDE-constrained optimization problem using standard nonlinear programming tools.

III. DISCRETIZATION TO A NONLINEAR PROGRAM

We create a discretization scheme to balance the high nonlinearity in the spatiotemporal dynamics (4)-(5) among a collection of auxiliary variables in which the constraints in Problem (18) possess a sparse representation.

For each pipe $P_{ij} \in \mathcal{P} - \mathcal{C}$, we create a set of $M+1$ time points t_m^{ij} and $N_{ij} + 1$ space points x_n^{ij} defined by

$$t_m^{ij} = m\Delta_{ij}^t, \quad m = 0, 1, \dots, M, \quad (19)$$

$$x_n^{ij} = n\Delta_{ij}^x, \quad m = 0, 1, \dots, N_{ij}, \quad (20)$$

$$\Delta_{ij}^t = \frac{T_{ij}}{M}, \quad \Delta_{ij}^x = \frac{L_{ij}}{N_{ij}}. \quad (21)$$

Here Δ_{ij}^t and Δ_{ij}^x are (dimensionless) time and space discretization steps, and T_{ij} is the dimensionless time horizon for pipe P_{ij} obtained from T according to (3). We omit the subscripts $\{ij\}$ on N_{ij} when they are clear from the context. For each of $(M+1) \times (N_{ij} + 1)$ discrete points in $\{(t_m, x_n) : 0 \le m \le M, 0 \le n \le N_{ij}\}$ within the (dimensionless) domain $[0, T_{ij}] \times [0, L_{ij}]$ for the flow dynamics on a pipe P_{ij}, we define

$$p_{ij}^{mn} \approx p_{ij}(t_m, x_n), \quad q_{ij}^{mn} \approx q_{ij}(t_m, x_n) \quad (22)$$

to be the pressure and mass flow variables at time $t = t_m$ and location $x = x_n$. We also define temporal and spatial

derivative variables at time $t = t_m$ and location $x = x_n$ by

$$pt_{ij}^{mn} \approx \frac{\partial p_{ij}}{\partial t}(t_m, x_n), \quad px_{ij}^{mn} \approx \frac{\partial p_{ij}}{\partial x}(t_m, x_n), \quad (23)$$

$$qx_{ij}^{mn} \approx \frac{\partial q_{ij}}{\partial x}(t_m, x_n). \quad (24)$$

A constraint that relates the discrete variables (22) to their derivatives (23)-(24) is created by approximating the integral over a time or space step by the trapezoid rule. This yields

$$\forall P_{ij} \in \mathcal{P} - \mathcal{C}, 0 \leq m \leq M - 1, 0 \leq n \leq N :$$

$$p_{ij}^{m+1,n} - p_{ij}^{mn} \approx \frac{\Delta_{ij}^t}{2}(pt_{ij}^{m+1,n} + pt_{ij}^{mn}) \quad (25)$$

$$\forall P_{ij} \in \mathcal{P} - \mathcal{C}, 0 \leq m \leq M, 0 \leq n \leq N - 1 :$$

$$p_{ij}^{m,n+1} - p_{ij}^{mn} \approx \frac{\Delta_{ij}^x}{2}(px_{ij}^{m,n+1} + px_{ij}^{mn}) \quad (26)$$

$$q_{ij}^{m,n+1} - q_{ij}^{mn} \approx \frac{\Delta_{ij}^x}{2}(qx_{ij}^{m,n+1} + qx_{ij}^{mn}) \quad (27)$$

The nondimensional dynamic equations (4)-(5) are then discretized in the above variables according to

$$\forall P_{ij} \in P - C, 0 \leq m \leq M, 0 \leq n \leq N :$$

$$pt_{ij}^{mn} + qx_{ij}^{mn} = 0 \quad (28)$$

$$2p_{ij}^{mn} px_{ij}^{mn} + q_{ij}^{mn}|q_{ij}^{mn}| = 0 \quad (29)$$

For each pipe $P_{ij} \in \mathcal{C}$, we define the discrete compression variables R_{ij}^m for $m = 0, 1, \ldots, M$, and suppose that the compressor is located at $c_{ij} = x_k$ for some $0 \leq k \leq N$, where the dependence of k on the pipe P_{ij} in question is clear from the context. The pipe is then divided into two pipes P_{iju} and P_{ijl}, with non-dimensional lengths L_{iju} and L_{ijl}, and for which we we define discrete variables

$$p_{iju}^{mn} \approx p_{ij}(t_m, x_n), q_{iju}^{mn} \approx q_{ij}(t_m, x_n), \ 0 \leq n \leq k \quad (30)$$

$$p_{ijl}^{mn} \approx p_{ij}(t_m, x_n), q_{ijl}^{mn} \approx q_{ij}(t_m, x_n), \ k \leq n \leq N \quad (31)$$

and corresponding spatial derivative variables $pt_{iju}^{mn}, px_{iju}^{mn}$, and qx_{iju}^{mn} for $0 \leq n \leq k$ and $pt_{ijl}^{mn}, px_{ijl}^{mn}$, and qx_{ijl}^{mn} for $k \leq n \leq N$. These state and derivative variables satisfy

$$p_{iju}^{m+1,n} - p_{iju}^{mn} \approx \frac{\Delta_{ij}^t}{2}(pt_{iju}^{m+1,n} + pt_{iju}^{mn}), \ 0 \leq n \leq k, \quad (32)$$

$$p_{ijl}^{m+1,n} - p_{ijl}^{mn} \approx \frac{\Delta_{ij}^t}{2}(pt_{ijl}^{m+1,n} + pt_{ijl}^{mn}), \ k \leq n \leq N \quad (33)$$

for $P_{ij} \in \mathcal{C}$ and $0 \leq m \leq M - 1$, and

$$p_{iju}^{m,n+1} - p_{iju}^{mn} \approx \frac{\Delta_{ij}^x}{2}(px_{iju}^{m,n+1} + px_{iju}^{mn}), \ 0 \leq n < k, \quad (34)$$

$$p_{ijl}^{m,n+1} - p_{ijl}^{mn} \approx \frac{\Delta_{ij}^x}{2}(px_{ijl}^{m,n+1} + px_{ijl}^{mn}), \ k \leq n \leq N, \quad (35)$$

$$q_{iju}^{m,n+1} - q_{iju}^{mn} \approx \frac{\Delta_{ij}^x}{2}(qx_{iju}^{m,n+1} + qx_{iju}^{mn}), \ 0 \leq n < k, \quad (36)$$

$$q_{ijl}^{m,n+1} - q_{ijl}^{mn} \approx \frac{\Delta_{ij}^x}{2}(qx_{ijl}^{m,n+1} + qx_{ijl}^{mn}), \ k \leq n \leq N \quad (37)$$

for $P_{ij} \in \mathcal{C}$ and $0 \leq m \leq M$. In addition, we require continuity constraints at the compressor location to connect

pipes P_{iju} and P_{ijl}, which take the form

$$R_{ij}^m = \frac{p_{ijl}^{mk}}{p_{iju}^{mk}}, \ q_{ijl}^{mk} = q_{iju}^{mk}, \quad (38)$$

for all $P_{ij} \in \mathcal{C}$ and $0 \leq m \leq M$. The equations (4)-(5) on either side of the compressor are discretized for $P_{ij} \in \mathcal{C}$ by

$$pt_{iju}^{mn} + qx_{iju}^{mn} = 0, \ 0 \leq n \leq k, \quad (39)$$

$$2p_{iju}^{mn} px_{iju}^{mn} + q_{iju}^{mn}|q_{iju}^{mn}| = 0, \ 0 \leq n \leq k, \quad (40)$$

$$pt_{ijl}^{mn} + qx_{ijl}^{mn} = 0, \ k \leq n \leq N \quad (41)$$

$$2p_{ijl}^{mn} px_{ijl}^{mn} + q_{ijl}^{mn}|q_{ijl}^{mn}| = 0, \ k \leq n \leq N \quad (42)$$

for all $P_{ij} \in \mathcal{C}$ and $0 \leq m \leq M$. The equations (25)-(29) and (32)-(42) discretize the dynamic equations (4)-(5) and continuity conditions for compressors (7)-(8). The pressure variables must also satisfy for all $0 \leq m \leq M$ the constraints

$$\underline{p}_{ij} \leq p_{ij}^{nm} \leq \overline{p}_{ij}, \quad P_{ij} \in P - C, 0 \leq n \leq N, \quad (43)$$

$$\underline{p}_{ij} \leq p_{iju}^{nm} \leq \overline{p}_{ij}, \quad P_{ij} \in C, 0 \leq n \leq k, \quad (44)$$

$$\underline{p}_{ij} \leq p_{ijl}^{nm} \leq \overline{p}_{ij}, \quad P_{ij} \in C, k \leq n \leq N \quad (45)$$

which discretize (6). In addition, the compression ratio must satisfy

$$\max\{\underline{R}_{ij}, 1\} \leq R_{ij}^m \leq \overline{R}_{ij}. \quad (46)$$

for $P_{ij} \in \mathcal{C}$ and $0 \leq m \leq M$. The cost of compression is then expressed by a constraint

$$S_{ij}^m = \eta^{-1} qm_{ij}^m((R_{ij}^m)^{2K} - 1) \quad (47)$$

for $P_{ij} \in \mathcal{C}$ and $0 \leq m \leq M$, where qm_{ij}^m is an auxiliary variable with the constraints

$$qm_{ij}^m \geq q_{iju}^{mk}, \quad qm_{ij}^m \geq -q_{iju}^{mk}, \quad (48)$$

so that $qm_{ij}^m = |q_{iju}^{mk}|$ when $R_{ij}^m > 1$. Compressor cost is also constrained to be positive, i.e.,

$$S_{ij}^m \geq 0. \quad (49)$$

The balance conditions at joints are given in the discrete variables for all $0 \leq m \leq M$ and $J_j \in \mathcal{J}$ by

$$\sum_{J_i \in \mathcal{J}: P_{ij} \in \mathcal{P}} q_{ij}^{mN} - \sum_{J_k \in \mathcal{J}: P_{jk} \in \mathcal{P}} q_{jk}^{m0} \quad (50)$$

$$+ \sum_{J_i \in \mathcal{J}: P_{ij} \in \mathcal{P}} q_{ijl}^{mN} - \sum_{J_k \in \mathcal{J}: P_{jk} \in \mathcal{P}} q_{jku}^{m0} = f_j^m,$$

and

$$p_{ij}^{mN} = p_j^m = p_{jk}^{m0}, \ \forall J_i, J_k \in \mathcal{J} \text{ s.t. } P_{ij}, P_{jk} \in \mathcal{P}. \quad (51)$$

Parametrization of these balance conditions for $0 \leq m \leq M$ is given by

$$f_i^m = d_i(t_m), \qquad J_i \in \mathcal{J} - \mathcal{S}, \quad (52)$$

$$p_i^m = s_i(t_m), \qquad J_i \in \mathcal{S}, \quad (53)$$

where $d_i(t)$ and $s_i(t)$ are given flow injection or supply pressure functions. The time-periodic boundary conditions on the states and controls are given for $0 \leq m \leq M$ by

$$p_{ij}^{0n} = p_{ij}^{Mn}, \qquad \forall P_{ij} \in \mathcal{P} - \mathcal{C}, 0 \leq n \leq N \qquad (54)$$

$$p_{iju}^{0n} = p_{iju}^{Mn} \qquad \forall P_{ij} \in \mathcal{C}, 0 \leq n \leq k \qquad (55)$$

$$p_{ijl}^{0n} = p_{ijl}^{Mn} \qquad \forall P_{ij} \in \mathcal{C}, k \leq n \leq N \qquad (56)$$

$$R_{ij}^0 = R_{ij}^M \qquad \forall P_{ij} \in \mathcal{C}. \qquad (57)$$

The integral in the objective of problem (18) is approximated by a Riemann sum (normalized by T) of the form

$$C_1 \approx \sum_{P_{ij} \in \mathcal{C}} \sum_{m=0}^{M} \frac{1}{M+1} S_{ij}^m. \qquad (58)$$

Finally, we add to the objective a penalty on total squared variation of compressor ratio values, in order to guarantee a physically realistic solution of the nonlinear program. This penalty takes the form

$$C_2 \approx \sum_{P_{ij} \in \mathcal{C}} \sum_{m=0}^{M-1} \frac{1}{M} (R_{ij}^m - R_{ij}^{m+1})^2. \qquad (59)$$

The nonlinear program is then given by

$$
\begin{aligned}
\min \quad & C_1 + \mu C_2 \text{ using } (58), (59) \\
s.t. \quad & \text{pipe dynamics: } (25) - (29) \ \& \ (32) - (42) \\
& \text{joint conditions: } (50), (51) \\
& \text{density \& compression constraints: } (43) - (46) \quad (60) \\
& \text{periodicity constraints: } (54) - (57) \\
& \text{injection parameters: } (52), (53) \\
& \text{compressor power: } (47) - (49)
\end{aligned}
$$

where μ is an appropriate scaling factor. The software implementation of this nonlinear programming approach is described in the next section, followed by descriptions of computational experiments involving several examples with comparisons to the results of other studies.

IV. IMPLEMENTATION AND EXAMPLES

Instead of solving the above nonlinear program directly, the implementation employs a lexicographic strategy. It first solves the nonlinear program with the original objective (58). It then solves the nonlinear program with the smoothness objective (59), while imposing the additional constraint

$$C_1 \leq (1+r)f, \text{ where } 0 \leq r \leq 1 \qquad (61)$$

where f is the optimal objective value of the first step. Intuitively, the tolerance r is a user-adjustable parameter that quantifies the percentage of compression energy that can be traded for a smoother solution. Note also that the second optimization stage is initialized using the first-stage solution.

This large-scale nonlinear problem is modeled with AMPL (version 2014) [34], [35] and solved with the nonlinear solver IPOPT 3.12.2, ASL routine (version 2015) [31]. The implementation is run on a Dell PowerEdge R415 with AMD Opteron 4226 and 64 GB ram.

We present the computational results of three case studies that include a validation of the proposed approach, as well as results about its solution quality, efficiency, and scalability.
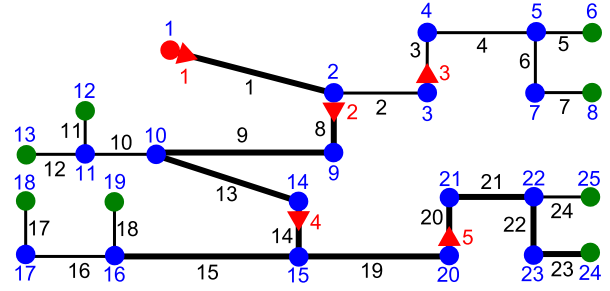
Fig. 1. 24-pipe gas system test network used in the benchmark case study. Numbers indicate nodes (blue), edges (black), and compressors (red). Thick and thin lines indicate 36 and 25 inch pipes. Nodes are source (red), transit (blue), and consumers (green).

a) Validation: The solution obtained using our implementation was validated on the 24-pipe benchmark gas network used in prior work [30], and illustrated in Figure 1. The pressures at supply sources were fixed at 500psi, the scalings for non-dimensionalization were set to $p_N = 250$psi and $q_N = 100$ kg/m^2/s, physical parameters $a = 377.968$ m/s, $\gamma = 2.5$, and $\lambda = 0.01$ were used, and a time horizon $T = 86400$ seconds (24 hours) was considered. Parameters D_{ij}, A_{ij}, L_{ij}, $\overline{R_{ij}}$, and $\underline{R_{ij}}$ were set according to the benchmark case study, as well as time-dependent profiles of gas injections/withdrawals $d_i(t)$. The benchmark network structure and the gas draw profiles are provided online [36]. Each pipe P_{ij} is discretized uniformly according to its length L_{ij} into $\lceil L_{ij}/E \rceil + 1$ segments, where E is set to 10km by default. In order to correspond to the structure of the benchmark model, the compressors are placed on the first segment of the ith end of every pipe $P_{ij} \in \mathcal{C}$.

The admissible pressure range is 500 to 800 psi throughout the network. A feasible solution to the discretized problem that satisfies the pressure constraints may cause these constraints to be violated in a high-accuracy simulation of the dynamics for the continuous problem. To address this issue, one version of our implementation tightens the pressure bounds conservatively by 4% or less, i.e. 520 to 780 psi for the benchmark case. We refer to this as "tightened", and optimization using the nominal constraints of 500 to 800 psi is referred to as "regular".

The optimization results were validated by using the optimized compression ratio solution as a time-varying parameter in a validated dynamic simulation method [32], [33], and through comparison to a state-of-the-art (benchmark) solution based on a pseudospectral discretization approach [30]. The trajectories computed using the simulation are used to validate the optimization solution in two ways. First, we quantify how much the constraints on pressure are exceeded by evaluating the L_2 norm of the violation. This aggregates violations over the 24-hour period by integrating the square of pressure violation (psi) of the bounds at every junction. This takes the form

$$v_p = \sqrt{\sum_{P_{ij} \in \mathcal{P}} V_{ij}^p} \qquad (62)$$
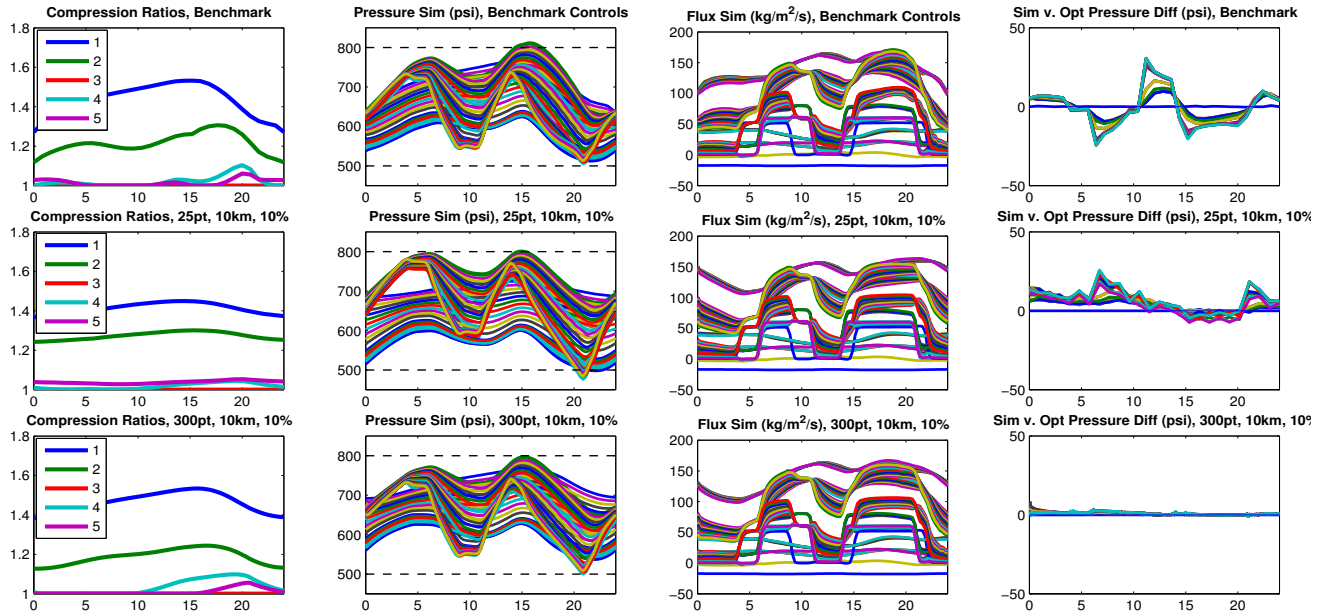
Fig. 2. From top to bottom: Benchmark solution; New method with 25 points in time, tightened constraints, 10km in space, $r = 10\%$; New method with 300 points in time, regular constraints, 10km in space, $r = 10\%$. From left to right: Optimal control solution; Pressure trajectories from simulation using the controls; Flux trajectories from the same simulation; Difference between pressure solution from optimization and pressure trajectories from simulation.

where

$$V_{ij}^p = \left[\int_0^T ((p_{ij}(t,0) - p_{\max})_+)^2 \mathrm{d}t \right]^{\frac{1}{2}}$$
$$+ \left[\int_0^T ((p_{\min} - p_{ij}(t,L_{ij}))_+)^2 \mathrm{d}t \right]^{\frac{1}{2}} \quad (63)$$

and $(x)_+ = x$ if $x \geq 0$ and $(x)_+ \equiv 0$ if $x < 0$. The unit of the metric is psi-days. Table I lists its values for solutions obtained using various time discretization M, smoothing parameter r, and using tightened and regular constraints. With the tightened bounds, the optimization solution has no, or very small violations for these configurations. Figure 2 depicts the optimal compressor ratio functions for 25 and 300 point temporal discretization, with tightened and regular constraints, respectively, and both with $E = 10$km spatial discretization and $r = 10\%$. A comparison is made with the solution to the same network obtained from prior work [30]. The smoothness of the compressor ratios over time indicates that the optimization solution is physically realistic and the control profiles can be implemented by operators. These results suggest that our optimization method provides operationally feasible solutions.

Next, we further validate the solutions provided by the solver by comparing the optimized pressure profiles with pressure trajectories obtained by applying the optimal controls in a dynamic simulation of the ODE model of the network [30] using an adaptive time-stepping solver `ode15s` in MATLAB. Figure 2 depicts the pressure and flow profiles resulting from the simulation, and the difference between optimization and simulation pressure trajectories is illustrated. For the 25 point time discretization, the discrepancy is similar to that for the benchmark solution, and using a 300 point time

TABLE I
AGGREGATED PRESSURE BOUND VIOLATIONS (v_p, PSI-DAYS).

Bounds	Tightened		Regular	
Time pt.	5%	10%	5%	10%
TZ 25tp	0.032	0.038	0.983	0.978
TZ 50tp	0.000	0.000	0.159	0.112
TZ 100tp	0.000	0.000	0.033	0.020
TZ 300tp	0.000	0.000	0.002	0.005
benchmark				0.9696

discretization nearly eliminates this difference. Because the sources of the compared pressure profiles are qualitatively very different, i.e., optimization of algebraic equations that discretize PDEs over a fixed grid compared with adaptive time-stepping solution of an ODE system, this is a powerful cross-validation of both models.

Finally, Table II presents the aggregated differences (in relative L2-Norm) between compressor ratios of the proposed method and the state-of-the-art benchmark solution. Specifically, we compute

$$v_R = \sqrt{\sum_{P_{ij} \in \mathcal{C}} (V_{ij}^R)^2} \quad (64)$$

where

$$V_{ij}^R = \frac{\int_0^T (R_{ij}(t) - R_{ij}^*(t))^2 \mathrm{d}t}{\int_0^T (R_{ij}^*(t))^2 \mathrm{d}t}. \quad (65)$$

Once again, the results indicate that the proposed method and the state-of-the-art yield highly similar compressor ratios across the network.

TABLE II

DISTANCE (v_R) OF COMPRESSION RATIOS W.R.T. BENCHMARKS

Bounds	Tightened		Regular	
Time pt.	5%	10%	5%	10%
TZ 25tp	0.002	0.004	0.002	0.004
TZ 50tp	0.002	0.004	0.003	0.004
TZ 100tp	0.002	0.004	0.002	0.003
TZ 300tp	0.003	0.004	0.000	0.001

TABLE III

OBJECTIVE VALUE (C_1) AND RUNTIMES ON 24 PIPE NETWORK.

TZ tp	Variables	Objective Value			CPU Time (secs)		
		1st Stage	2nd Stage		1st Stage	2nd Stage	
			$r = 5\%$	10%		$r = 5\%$	10%
25	11,675	2.024	2.126	2.227	10	20	25
40	18,410	2.067	2.170	2.273	21	47	65
50	22,900	2.120	2.226	2.332	23	120	34
60	27,390	2.133	2.239	2.346	47	227	61
80	36,370	2.134	2.240	2.347	109	209	97
100	45,350	2.130	2.237	2.343	158	375	100
300	135,150	2.132	2.238	2.345	1,089	429	378
Benchmark	3937	2.2752			112*		

TABLE IV

OBJECTIVE VALUE (C_1) AND RUNTIMES ON 40 PIPE NETWORK.

TZ tp	Variables	Objective Value			CPU Time (secs)		
		1st Stage	2nd Stage		1st Stage	2nd Stage	
			$r = 5\%$	10%		$r = 5\%$	10%
20	20,875	1.238	1.300	1.362	51	19	62
25	25,845	1.274	1.337	1.401	71	51	53
40	40,755	1.257	1.320	1.383	353	256	270

TABLE V

OBJECTIVE VALUE (C_1) AND RUNTIMES ON 135 PIPE NETWORK.

TZ tp	Variables	Objective Value			CPU Time (secs)		
		1st Stage	2nd Stage		1st Stage	2nd Stage	
			$r = 5\%$	7%		$r = 5\%$	7%
10	56,618	4.048	4.250	4.331	3,547	388	194
15	82,353	6.760	7.098	7.233	3,974	722	1,190
20	108,088	7.945	8.342	8.501	13,726	2,599	1,761
25	133,823	7.307	7.672	7.818	22,024	1,987	2,225
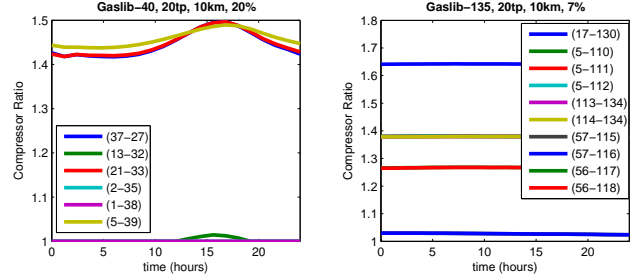
Fig. 3. Compression ratio solutions for gaslib-40 (left) and gaslib-135 (right) case studies. The trapezoidal scheme is used for time discretization with 20 points, and the smoothness tolerances are $r = 10\%$ and $r = 7\%$, respectively.

c) Scalability: To study how the proposed method scales to larger network models, two additional instances are considered: gaslib-40 and gaslib-135 from the GasLib library [37]. The admissible pressure range is $[500, 1000]$ psi for both the gaslib-40 and gaslib-135 instances, and the source pressure is set to 650 and 600 psi respectively. Simplified network structures and time-dependent gas draw profiles are provided online [36]. Tables IV and V present the results, which show that the proposed method scales well to larger benchmarks and exhibits similar behavior as on the 24-pipe network. The 40 pipe network is solved in less than two minutes, and the 135 pipe network in around an hour. Figure 3 presents the smoothness results for these two case studies. Only a subset of the compressors are shown for these cases.

V. CONCLUSIONS

We have investigated the Dynamic Optimal Gas Flow (DOGF) problem in which the goal is to minimize compressor costs under dynamic conditions where deliveries to customers are described by time-dependent mass flow functions. This study is motivated by the growing reliance of electric power systems on gas-fired generation in order to balance intermittent sources of renewable energy. This deeper integration has increased the variation and volume of flows through natural gas transmission pipelines, emphasizing the need to go beyond steady-state optimization in controlling and optimizing natural gas networks. Maintaining efficiency and security under such dynamic conditions requires optimization methods that account for transients and can quickly compute solutions to follow generator re-dispatch.

This paper presents an efficient scheme for the DOGF that relies on a compact representation of gas flow physics and a trapezoidal discretization in time and space that allows sparse representation of constraints. A two-stage approach is

b) Solution Quality and Efficiency: Table III reports the objective value C_1 and computation time of the proposed method for various time discretizations and smoothness parameters r. The number of variables in the optimization problem ranges from 11,675 for the 25pt discretization to 135,150 for the 300pt model. The table gives the value of the C_1 objective after the first stage, and also in the second stage for $r = 5\%$ and 10%. The CPU times in seconds for the first and second stages are also reported. First, we observe that enforcing the smoothness of the solution does not fundamentally decrease the quality of the C_1 objective, which is important from an operational standpoint. Second, as expected, refining the time discretization increases the objective value, because more constraints are added. The convergence rate is fast and the solutions obtained with a coarse discretization are already of high quality, as illustrated in Figure 2. Finally, the method is efficient; consider the time granularities with 25 and 40 points: For $r = 10\%$, the method takes about 30 and 80 seconds, respectively, which indicates that it can be used during real-time operations. The last line describes the objective value and the execution of the state-of the art (benchmark) solution [30], which was executed on a different machine, and only given to indicate that our implementation is comparable to previous work.

applied to minimize energy costs and maximize smoothness to correspond to physically correct solutions. The resulting large-scale nonlinear programs are solved using a modern interior-point method and the results are validated using an accurate simulation of the dynamic equations and a recently proposed state-of-the-art method. The novel optimization scheme yields solutions that are feasible for the continuous problem and practical from an operational standpoint in a computation time that is up to an order of magnitude faster than existing methods. Scalability of the scheme is demonstrated using three networks with 24, 40, and 135 pipes with total lengths of 477, 1118, and 6964 km of pipeline, respectively. Future work will further accelerate computation by exploiting the underlying time structure of the optimization problem as suggested in [38], and by considering alternative discretization schemes and how they impact accuracy and performance.

REFERENCES

[1] C. Lyons and G. Litra. Gas-power interdependence: Knock-on effects of the dash to gas, 2013.

[2] T. Li, M. Eremia, and M. Shahidehpour. Interdependency of natural gas network and power system security. *IEEE Transactions on Power Systems*, 23(4):1817–1824, 2008.

[3] MITEI. Growing concerns, possible solutions: The Interdependency of Natural Gas and Electricity Systems, 2013. http://mitei.mit.edu/publications/reports-studies/growing-concerns-possible-solutions.

[4] M. Chertkov, S. Backhaus, and V. Lebedev. Cascading of fluctuations in interdependent energy infrastructures: Gas-grid coupling. *arxiv:1411.2111*, 2014.

[5] C. Luongo, W. Yeung, and B. Gilmour. Optimizing the operation of gas transmission networks. In *Computers in engineering 1991*, 1991.

[6] R. Z. Ríos-Mercado and C. Borraz-Sánchez. Optimization problems in natural gas transportation systems: A state-of-the-art review. *Applied Energy*, 147:536–555, 2015.

[7] P. Wong and R. Larson. Optimization of natural-gas pipeline systems via dynamic programming. *Automatic Control, IEEE Transactions on*, 13(5):475–481, 1968.

[8] B. Rothfarb, H. Frank, D. M. Rosenbaum, K. Steiglitz, and D. J. Kleitman. Optimal design of offshore natural-gas pipeline systems. *Operations research*, 18(6):992–1020, 1970.

[9] K. T. Midthun, M. Bjørndal, and A. Tomasgard. Modeling optimal economic dispatch and system effects in natural gas networks. *The Energy Journal*, pages 155–180, 2009.

[10] C. Borraz-Sanchez. *Optimization methods for pipeline transportation of natural gas*. PhD thesis, Bergen Univ.(Norway), 2010.

[11] S. Misra, M. W. Fisher, S. Backhaus, R. Bent, M. Chertkov, and F. Pan. Optimal compression in natural gas networks: A geometric programming approach. *IEEE Transactions on Control of Network Systems*, 2(1):47–56, 2015.

[12] F. Babonneau, Y. Nesterov, and J.-P. Vial. Design and operations of gas transmission networks. *Operations research*, 60(1):34–47, 2014.

[13] C. Borraz-Sanchez, R. Bent, S. Backhaus, H. Hijazi, and P. Van Hentenryck. Convex relaxations for gas expansion planning. *arXiv preprint arXiv:1506.07214*, 2015.

[14] G. L. Peters. Gas and Electric Infrastructure Interdependency Analysis. *Envision Energy Solutions*, 22, 2012.

[15] G. L. Peters. Embedded natural gas-fired electric power generation infrastructure analysis: An analysis of daily pipeline capacity availability. Technical report, EnVision Energy Solutions, 2012.

[16] M. Chertkov, M. Fisher, S. Backhaus, R. Bent, and S. Misra. Pressure fluctuations in natural gas networks caused by gas-electric coupling. In *48th Hawaii International Conference on System Sciences (HICSS)*, pages 2738–2747. IEEE, 2015.

[17] R. Levitan et al. Pipeline to reliability: Unraveling gas and electric interdependencies across the eastern interconnection. *Power and Energy Magazine, IEEE*, 12(6):78–88, 2014.

[18] M. Shahidehpour and Z. Li. White paper: Long-term electric and natural gas infrastructure requirements. Technical report, llinois Institute of Technology, 2014.

[19] Forward Market Operations. Energy & Ancillary Services Market Operations, M-11 Rev. 75. Technical report, PJM, 2015.

[20] E. Litvinov. Design and operation of the locational marginal prices-based electricity markets. *Generation, Transmission Distribution, IET*, 4(2):315–323, February 2010.

[21] H. Hijazi, T. Mak, and P. Van Hentenryck. Power system restoration with transient stability. In *Proceedings of the Twenty-Ninth AAAI Conference on Artificial Intelligence*, Austin, Texas, 2015.

[22] P. Van Hentenryck and C. Coffrin. Transmission system repair and restoration. *Mathematical Programming*, 151(1):347–373, 2015.

[23] A. Osiadacz. Simulation of transient gas flows in networks. *International J. for Numerical Methods in Fluids*, 4:13–24, 1984.

[24] M. Herty et al. A new model for gas flow in pipe networks. *Math. Methods in the Applied Sci.*, 33(7):845–855, 2010.

[25] A. Thorley and C. Tiley. Unsteady and transient flow of compressible fluids in pipelines – a review of theoretical and some experimental studies. *Internat. J. of Heat and Fluid Flow*, 8:3–15, 1987.

[26] H. Rachford and R. Carter. Optimizing pipeline control in transient gas flow. *Pipeline Simulation Interest Group*, 2000.

[27] K. Ehrhardt and M. Steinbach. *Nonlinear optimization in gas networks*. Springer, 2005.

[28] M. Steinbach. On PDE solution in transient optimization of gas networks. *J. of Computat. and Appl. Math.*, 203(2):345–361, 2007.

[29] V. Zavala. Stochastic optimal control model for natural gas networks. *Computers & Chemical Engineering*, 64:103–113, 2014.

[30] A. Zlotnik, M. Chertkov, and S. Backhaus. Optimal control of transient flow in natural gas networks. In *54th IEEE Conference on Decision and Control*, pages 4563–4570, Osaka, Japan, 2015.

[31] A. Wächter and L. T. Biegler. On the implementation of an interior-point filter line-search algorithm for large-scale nonlinear programming. *Mathematical Programming*, 106(1):25–57, 2006.

[32] S. Grundel, L. Jansen, N. Hornung, T. Clees, C. Tischendorf, and P. Benner. Model order reduction of differential algebraic equations arising from the simulation of gas transport networks. *Progress in Differential-Algebraic Equations*, 2013.

[33] A. Zlotnik, S. Dyachenko, S. Backhaus, and M. Chertkov. Model reduction and optimization of natural gas pipeline dynamics. In *ASME Dynamic Systems and Control Conference*, page V003T39A002, Columbus, OH, 2015.

[34] R. Fourer, D. M. Gay, and B. W. Kernighan. *AMPL: A Modeling Language for Mathematical Programming*. Cengage Learning, 2002.

[35] AMPL. AMPL Optimization: http://www.ampl.com, 2015.

[36] Gas pipeline system benchmark data; network structure and dynamic parameters. https://db.tt/PqZY3MCG.

[37] M. Pfetsch, A. Fügenschuh, B. Geißler, N. Geißler, R. Gollmer, B. Hiller, J. Humpola, T. Koch, T. Lehmann, A. Martin, A. Morsi, J. Rövekamp, L. Schewe, M Schmidt, R. Schultz, R. Schwarz, J. Schweiger, C. Stangl, M. Steinbach, S. Vigerske, and B. Willert. Validation of nominations in gas network optimization: Models, methods, and solutions. *Optimization Methods and Software*, 30(1):15–53, 2015.

[38] N. Chiang, C. G. Petra, and V. M. Zavala. Structured nonconvex optimization of large-scale energy systems using pips-nlp. In *Power Systems Computation Conference (PSCC'14)*, 2014.